

## Equilibrium Core Design for 170MWe PWR-Type SMR Applying a Two-Batch Fuel Management Concept

Dokyun Kim<sup>a</sup> and Hyung Jin Shim<sup>a\*</sup>

<sup>a</sup> Seoul National University, 1 Gwanak-ro, Gwanak-gu, Seoul 08826, Korea

\*Corresponding author: shimhj@snu.ac.kr

### 1. Introduction

Small modular reactors (SMRs) are considered to be a promising option due to their versatility, improved safety features, and cost-effectiveness [1]. One trend among these designs is the use of soluble boron-free (SBF) operation, which offers several benefits such as simplifying the core system, reducing the size of the nuclear power plant by eliminating the need for a chemical volume control system, reducing the amount of liquid radioactive waste, preventing the corrosion problem caused by boric acid, and maintaining the negative moderator temperature coefficient, thereby improving inherent safety [2].

Recently, a collaboration between universities, research institutes, industries, and government bodies has been driving the development of the conceptual design of a new type of SMR based on the pressurized water reactor (PWR) called i-SMR [3]. The main specifications for the i-SMR include a power output of 170MWe, the use of SBF operation, and a refueling cycle of over 24 months [4].

The purpose of this study is to design an equilibrium core for 170 MWe PWR-types SMR that meets specific design criteria, using a two-batch fuel management approach. The target of the refueling cycle and the limit of maximum excess reactivity are over 24 months and within 5,000 pcm, respectively. The 170 MWe SMR core is designed to produce 540 MW thermal power from 69 fuel assemblies (FAs) based on Westinghouse (WH) 17×17 using 4.95% enriched UO<sub>2</sub> fuel. Solid Pyrex rod is loaded into FA as a burnable absorber (BA) for reactivity control in SBF operation [5]. The two-batch refueling approach considers factors such as initial reactivity, cycle length, radial power distribution, and burnup of each FA to optimize the location of fresh and once-burned FA. For the core design, neutronics calculations are performed by the Monte Carlo particle transport analysis code, McCARD [6] with the ENDF/B-VII.1 cross-section library [7].

### 2. Core Description of 170MWe SMR

#### 2.1 Core design parameters

Table I shows the design parameters of 170MWe SMR. The core is composed of 69 FAs illustrated in Figure 1. Each assembly is based on WH 17×17 array loaded with 240 UO<sub>2</sub> fuel pins and 24 Pyrex pins as shown in Figure 2, and their arrangement was determined by referring to previous study [8]. Pyrex is a commercial name given to a type of borosilicate glass

that is composed of B<sub>2</sub>O<sub>3</sub>-SiO<sub>2</sub>. In SBF SMR core designs, the use of Pyrex BA enables effective control of initial excess reactivity and long cycle lengths [5, 8].

Table I: Design parameters of 170MWe SMR

Parameters	Value
Reactor type	PWR
Electric power	170 MWe
Thermal power	540 MWt
Number of FAs	69
Active core height (H)	240 cm
Equivalent diameter (D)	201.55 cm
D/H ratio	0.8398
Average linear power density	12.35 kW/m
FA type	WH 17×17
FA pitch / Pin pitch	21.50 cm / 1.26 cm
Uranium enrichment	4.95 wt.%
Fuel material	UO <sub>2</sub>
BA material	Solid Pyrex
Soluble boron	0 ppm
Target cycle length	> 24 months
Target Max. excess reactivity	< 5000 pcm

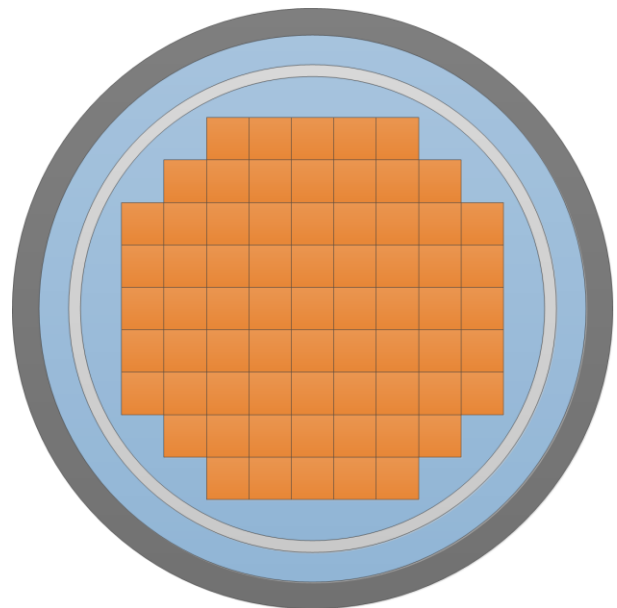


Fig. 1. 170MWe SMR core configuration

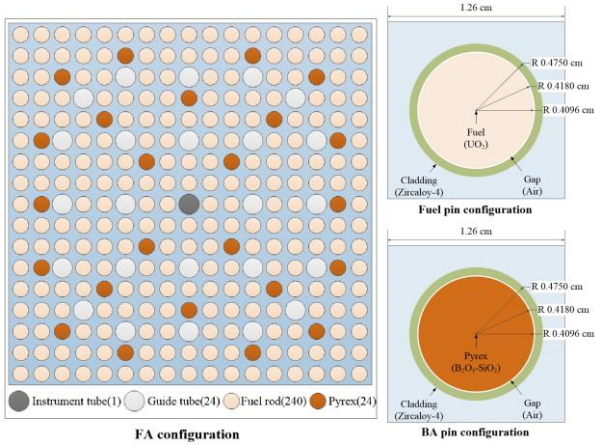


Fig. 2. FA configuration

## 2.2 Prediction of cycle length in a single-batch core

To estimate the cycle length of the 170 MWe SMR core, the McCARD burnup calculation was conducted for a single-batch core loading pattern. As shown in Figure 3, the core consisted of 5 types of FA with different concentrations of  $B_2O_3$  in Pyrex. FAs with high concentrations of  $B_2O_3$  were placed in the core's center, while assemblies with low concentrations were placed on the periphery to ensure a smooth power distribution in the radial direction. Table II presents the information of FA types by the concentration of BA.

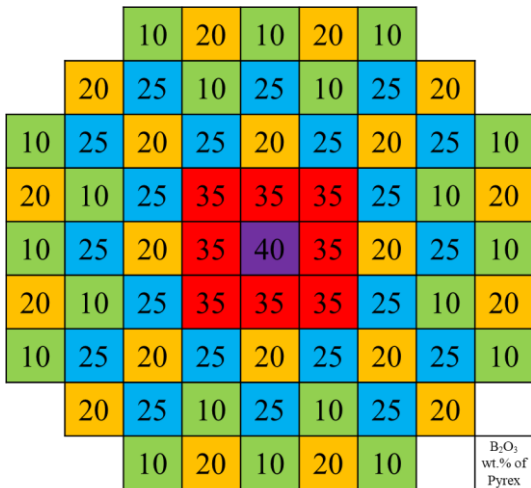


Fig. 3. Loading pattern of SMR

Table II: The information of FAs

$B_2O_3$ wt.% of Pyrex	Number of fuel pins	Number of BA pins	Number of FA
10	240	24	20
20	240	24	20
25	240	24	20
35	240	24	8
40	240	24	1
Total	16,560	1,656	69

The McCARD burnup calculation was performed with 50,000 histories per cycle on 150 inactive and 300 active cycles. Based on the results, the predicted cycle length for the 170 MWe SMR core was approximately 980 days, with a discharged burnup of 28 MWd/kgU and an initial excess reactivity of no more than 5,000 pcm. Figure 4 shows effective multiplication factor ( $k_{eff}$ ) versus effective full power day (EFPD) behavior with or without BA for single-batch core, and the standard deviation (SD) of  $k_{eff}$  is less than 0.00018.

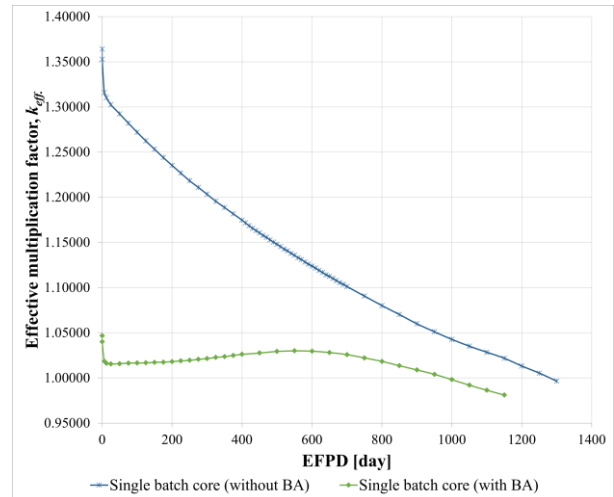


Fig. 4.  $k_{eff}$  vs. EFPD behavior with or without BA

## 3. Equilibrium core design applying 2-batch fuel management

### 3.1 Two-batch fuel management approach

To apply two-batch fuel management to the core design, 40 fresh FAs and 29 once-burned FAs are arranged in the core for each burnup cycle. To increase the discharged burnup of FAs and reduce radial power peaking, one single FA once burned is positioned at the center of the core, while the other 28 FAs once burned are reloaded into the peripheral region to reduce neutron leakage out of the core and extend the cycle length, as illustrated in Figure 5. Table III shows the reloading shuffling scheme used in the 2-batch core design.

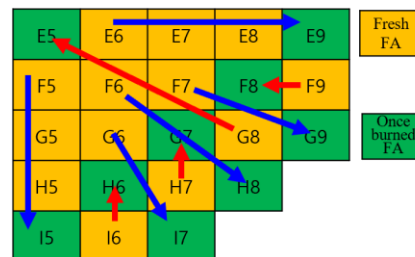


Fig. 5. Reloading pattern for 2-batch (1/4 core)

Table III: Reloading shuffling scheme for 2-batch.

Fresh FA		Once burned FA		Twice burned FA	No. of FA
E6	→	E9	→	Discharged	2
E7	→	Discharged	-	-	2
E8	→	Discharged	-	-	2
F5	→	I5	→	Discharged	2
F6	→	H8	→	Discharged	4
F7	→	G9	→	Discharged	4
F9	→	F8	→	Discharged	4
G5	→	Discharged	-	-	2
G6	→	I7	→	Discharged	4
H5	→	Discharged	-	-	2
H7	→	G7	→	Discharged	4
I6	→	H6	→	Discharged	4
G8	→	E5	→	Discharged	1
	→	Discharged	-	-	3

### 3.2 Equilibrium core loading patterns

As shown in Figure 5, loading pattern (LP) case 1 was designed in the proposed reloading shuffling scheme for 2-batch using FA loaded with only one type of Pyrex without considering the flattening of power distribution.

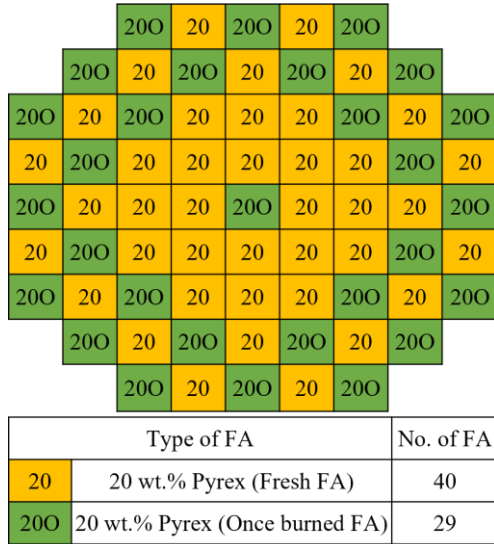


Fig. 6. LP Case 1 in the equilibrium core condition

To reduce the power peaking factor and extend the cycle length, LP Case 2 was designed to place fresh FAs with a high Pyrex concentration in the center of the core and fresh assemblies with a low Pyrex concentration at the periphery. The 29 FAs once burned are relocated in the proposed reloading shuffling scheme method for 2-batch. Figure 7 shows LP case 2 in the equilibrium core condition.

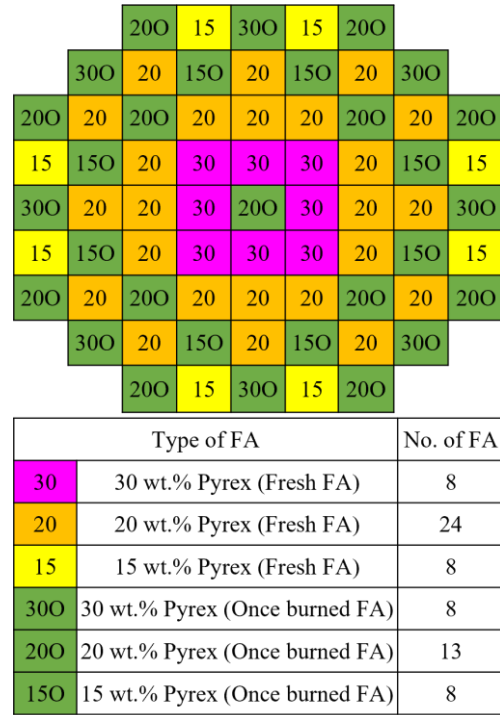


Fig. 7. LP Case 2 in the equilibrium core condition

## 4. Results

### 4.1 Equilibrium core cycle search

To find the equilibrium (Eq) core cycle, McCARD burnup calculations were performed as shown in Table IV. The end of the cycle (EOC) burnups of the previous cycle are taken to be 18.53 MWd/kgU (650 EFPD) and 19.96 MWd/kgU (700 EFPD), respectively. Figures 8 and 9 show  $k_{eff}$  versus EFPD behavior for each case. Based on the graphs presented, a similar tendency was observed starting from the 3<sup>rd</sup> cycle, and the cycle length and initial excess reactivity converge in the 4<sup>th</sup> cycle.

Table IV: McCARD burnup calculation options

Cycle		2 <sup>nd</sup> , 3 <sup>rd</sup> , 4 <sup>th</sup>	5 <sup>th</sup> (Eq cycle)
Neutron histories		20,000	50,000
Active/inactive cycle		300 / 150	300 / 150
SD of $k_{eff}$		< 0.00030	< 0.00020
Fuel avg. temperature		900 K	
Moderator avg. temperature		600 K	
EOC burnup of previous cycle	LP case 1	18.53 MWd/kgU (650 EFPD)	
	LP case 2	19.96 MWd/kgU (700 EFPD)	

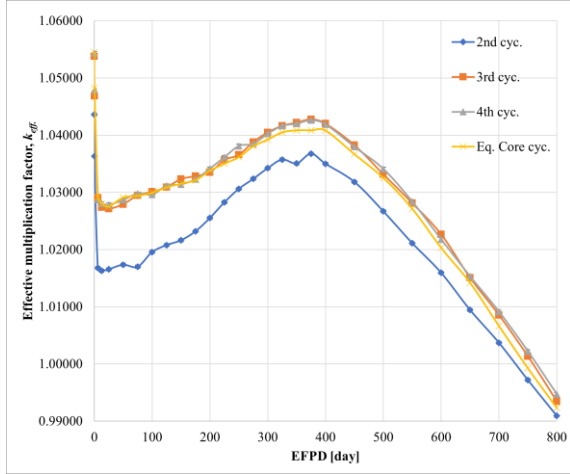


Fig. 8.  $k_{eff}$  vs. EFPD behavior for each cycle of LP case 1

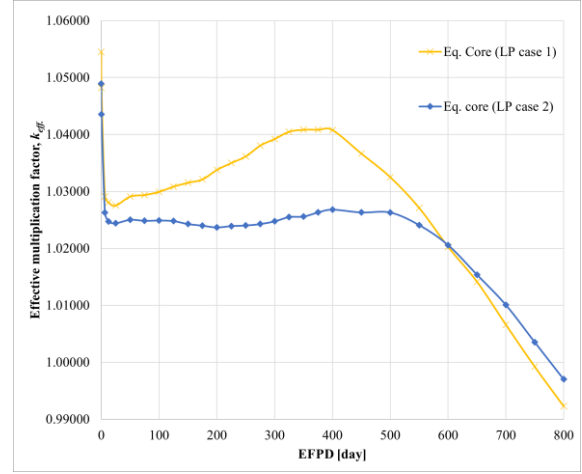


Fig. 10. Comparison of  $k_{eff}$  vs. EFPD behavior for both cores

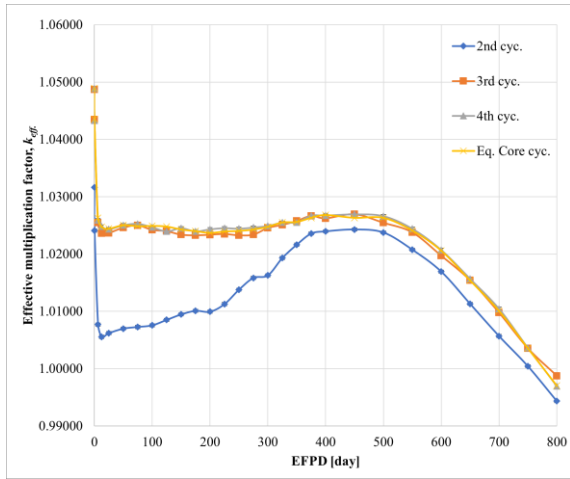


Fig. 9.  $k_{eff}$  vs. EFPD behavior for each cycle of LP case 2

#### 4.2 Comparison of both equilibrium cores

Figure 10 compares  $k_{eff}$  versus EFPD behavior for two cores. It was observed that LP case 2 had a smaller reactivity swing and greater safety margins compared to LP case 1. LP case 2 also exhibited a longer cycle length, with the initial excess reactivity being  $523 \pm 22$  pcm less than that of LP case 1. The maximum cycle lengths for LP case 1 and LP case 2 were calculated to be  $745 \pm 2$  and  $777 \pm 3$  days, respectively. Table V provides a comparison of both cores' characteristics, such as initial excess reactivity, excess reactivity after Eq Xenon, and cycle length.

Table V: Comparison of both cores' characteristics.

Division	LP case 1	LP case 2	Difference (LP2 – LP1)
Initial excess reactivity [pcm]	$5,168 \pm 16$	$4,663 \pm 16$	$- 523 \pm 22$
Excess reactivity after Eq Xenon [pcm]	$3,924 \pm 17$	$2,611 \pm 18$	$- 683 \pm 25$
Cycle length [day]	$745 \pm 2$	$777 \pm 3$	$+ 32 \pm 4$

The radial power distributions for both cores at the beginning of the cycle (BOC), 350 EFPD and EOC are illustrated in Figures 11 and 12, and the SD of the FA normalized power is less than 0.002. In both cores, the maximum radial FA power appeared at the core center at BOC, and as the cycle advanced, the power peak shifted from the inner core to the middle core region.

1.905	1.857	1.517	1.013	0.393
1.792	1.704	1.429	0.962	0.461
1.303	1.509	1.479	1.193	0.494
1.859	1.737	1.412	0.901	0.430
1.792	1.704	1.429	0.962	0.461
1.505	1.506	1.410	1.038	0.561
1.519	1.407	1.079	0.697	0.262
1.521	1.420	1.061	0.723	0.280
1.477	1.407	1.074	0.851	0.345
1.008	0.902	0.703	0.314	
1.049	0.958	0.722	0.324	
1.177	1.036	0.850	0.391	
0.391	0.428	0.264		0 EFPD
0.412	0.459	0.280		350 EFPD
0.489	0.561	0.344		650 EFPD

Fig. 11. Radial power distribution of LP case 1

1.533	1.499	1.458	1.136	0.510
1.406	1.387	1.410	1.093	0.599
1.337	1.529	1.466	1.160	0.520
1.495	1.459	1.396	1.077	0.558
1.406	1.387	1.410	1.093	0.599
1.531	1.505	1.391	1.000	0.595
1.452	1.397	1.145	0.809	0.326
1.458	1.408	1.124	0.839	0.349
1.476	1.400	1.030	0.835	0.345
1.125	1.066	0.805	0.376	
1.175	1.082	0.837	0.403	
1.180	1.004	0.837	0.396	
0.502	0.553	0.324		0 EFPD
0.532	0.591	0.347		350 EFPD
0.521	0.595	0.346		700 EFPD

Fig. 12. Radial power distribution of LP case 2

The maximum radial FA power (Max. FA power) versus EFPD for both cores is compared in Figure 12. With the exception of EOC, the Max. FA power values of LP case 1 were generally higher than those of LP case 2. It was observed that the Max. FA power behavior in LP case 1 tended to decrease rapidly from BOC to EOC, while LP case 2, it decreased from BOC to 150 EFPD and then gradually increased to EOC.

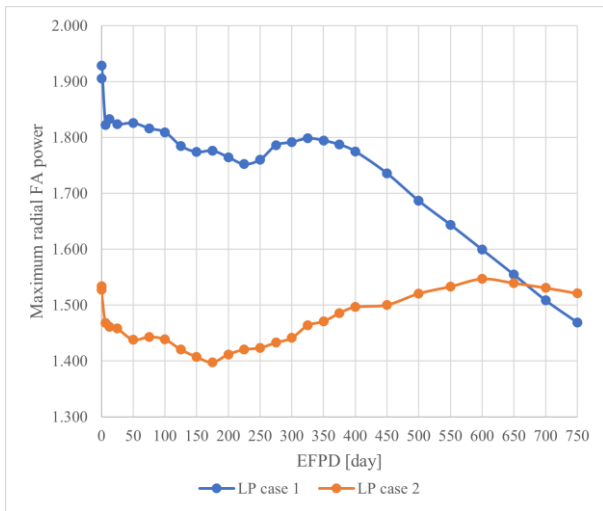


Fig. 13. Max. FA power vs. EFPD of both cores

Figure 14 displays the comparison of pin power peaking factor ( $F_q$ ) versus EFPD for LP case 1 and LP case 2. The SD of  $F_q$  was found to be less than 0.05. Both graphs exhibited a decreasing trend from BOC to EOC, with peak values of  $F_q$  observed at BOC. The maximum  $F_q$  value for LP case 1 was calculated to be  $3.33 \pm 0.04$ , whereas LP case 2 had a maximum  $F_q$  value of  $2.90 \pm 0.05$ . The results of this study indicate that LP case 2's Eq core had higher safety margins than that of LP case 1.

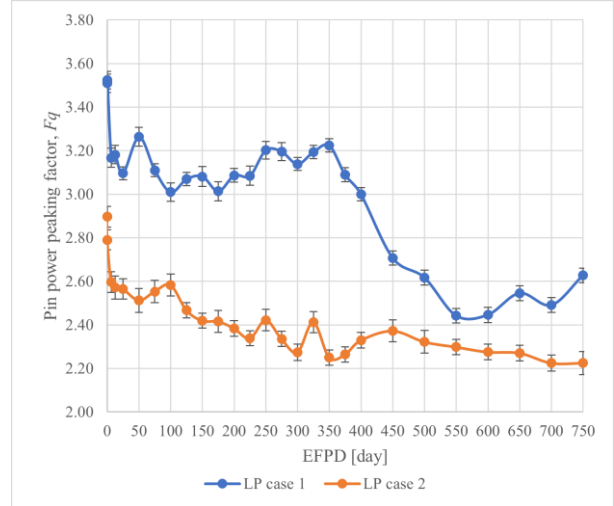


Fig. 14.  $F_q$  vs. EFPD of both cores

The normalized axial power distribution of both cores is shown in Figure 15. In this study, it should be noted that the depletion calculations were performed without considering the thermal-hydraulic feedback effect. It was observed that LP case 2 had a relatively flat axial power shape compared to LP case 1 at MOC and EOC.

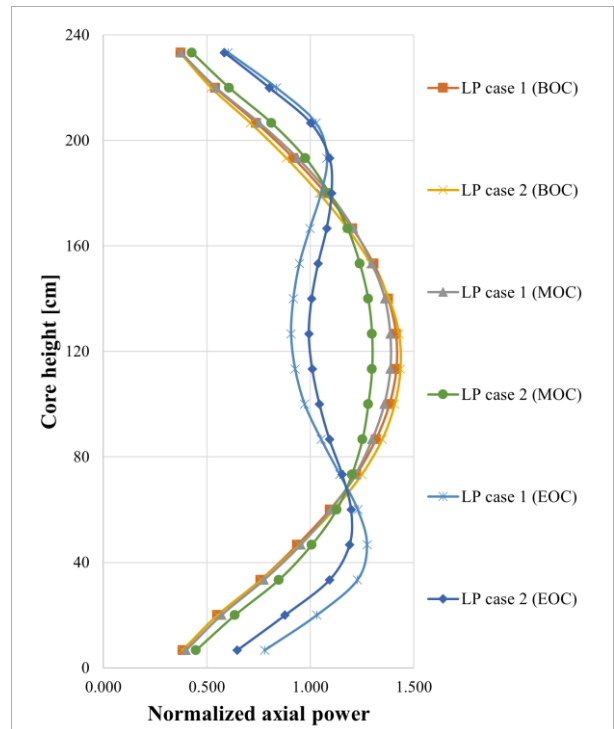


Fig. 15. Axial power distributions of both cores

Table VI summarizes the discharged burnups of FAs, indicating that LP case 2 achieved a higher discharged burnup ( $30.55 \text{ MWd/kgU}$ ) than LP case 1 ( $28.41 \text{ MWd/kgU}$ ). The increase in the average discharged burnup in LP Case 2 was attributed to achieving a

higher discharged burnup of FAs in the outer region of the core compared to LP case 1.

Table VI: Comparison of FA discharged burnups.

Fresh FA	No. of FA	Discharged burnup [MWd/kgU]		Relative difference * (LP2-LP1) / LP1
		LP case 1	LP case 2	
E6	2	30.45	30.64	+0.6%
E7	2	50.15	48.89	-2.5%
E8	2	19.88	23.33	+17.4%
F5	2	30.41	30.57	+0.5%
F6	4	27.59	27.77	+0.6%
F7	4	23.39	26.92	+15.1%
F9	4	24.15	30.07	+24.5%
G5	2	50.09	48.83	-2.5%
G6	4	13.97	16.75	+19.8%
H5	2	19.87	23.31	+17.3%
H7	4	29.73	34.30	+15.4%
I6	4	24.17	29.96	+24.0%
G8	1	39.86	39.58	-0.7%
G8	3	13.97	16.74	+19.9%
Average		28.41	30.55	+ 7.5%
* SD of FA discharged burnup < 0.20				

## 5. Conclusions

In this study, the equilibrium core design for 170 MWe SMR was presented using a 2-batch fuel management approach, where 40 fresh FAs were reloaded, and 29 assemblies were burned twice. Based on the results of the study, it was found that the equilibrium core cycle converged after the 4<sup>th</sup> burnup cycle, and the core design satisfied the desired requirements for the refueling cycle (> 24 months) and the excess reactivity (< 5,000 pcm). However, a limitation of this study is that the maximum  $Fq$  value for LP case 2 was  $2.90 \pm 0.05$ , indicating the need for optimization to decrease the power peak value.

In future work, to reduce power peaking factor and optimize the equilibrium core, we are considering several methods, such as applying axial cutback for BAs, utilizing a mixture of different types of BAs, and searching for an LP with a more flattened radial power distribution. In addition, it is expected that useful information on spent fuel can be obtained by analyzing the composition and amount of spent fuel from the SMR core compared to conventional PWRs.

## 6. Acknowledgements

This work was supported by the National Research Foundation of Korea (NRF) Grant funded by the Korean Government (MSIT) (NRF-2022M2BA109805911).

## REFERENCES

- [1] Advances in Small Modular Reactor Technology Developments (2020 Edition), International Atomic Energy Agency, A Supplement to: IAEA Advanced Reactors Information System (ARIS), September 2020.
- [2] Ingersoll, Daniel T., and Mario D. Carelli, eds. Handbook of small modular nuclear reactors. Woodhead Publishing, 2020.
- [3] Kwon, H., S. Y. Kima, and H. O. Kang, Lessons Learned from Development of NuScale NPP for Successful Standard Design Certification of i-SMR, Transactions of the Korean Nuclear Society Spring Meeting, Jeju, Korea, May 19-20, 2022.
- [4] 허선(2021.6.17). 혁신형 SMR 개발 및 추진 현황 [발표자료], 2021 원자력안전규제정보회의, 대전. <https://nsic.nssc.go.kr/information/nssc.do#>
- [5] Kim, Jinsun, et al, Use of solid pyrex rod for conceptual soluble boron free SMR, Transactions of the American Nuclear Society 11, 2016.
- [6] H. J. Shim, B. S. Han, J. S. Jung, H. J. Park, and C. H. Kim, McCARD: Monte Carlo code for advanced reactor design and analysis, Nucl. Eng. Technol., Vol. 44, No. 2, p. 161, 2012.
- [7] CHADWICK, Mark B., et al. ENDF/B-VII. 1 nuclear data for science and technology: cross sections, covariances, fission product yields and decay data. Nuclear data sheets, 2011, 112.12: 2887-2996.
- [8] Kim, D., 2021. Advanced Core Design of Soluble Boron Free Small Modular Reactor for Marine Applications, Master thesis, Seoul National University.